J Mater Sci: Mater Med (2009) 20:S181–S187
DOI 10.1007/s10856-008-3509-z

Nanostructured porous silicon as functionalized material for biosensor application

Shalini Singh · Shailesh N. Sharma · Govind · S. M. Shivaprasad · Mohan Lal · Mukhtar A. Khan

Received: 5 November 2007 / Accepted: 16 June 2008 / Published online: 3 July 2008

Abstract In this work by means of PL, FTIR and XPS techniques, state-of-the-art porous silicon (PS) films with good mechanical and optical properties have been effectively utilized for the biofunctionalization purpose for its possible application in immunosensors. The functionalization of the PS surface has been achieved by silanization process using aminopropyltriethoxysilane (APTS) as a precursor. The presence of reactive amino groups on the PS surface along with glutaraldehyde as a linker aids in the covalent binding of the antibody (Human IgG) onto the PS surface. Different antigen concentrations can be detected with a good reproducibility with this technique which opens a huge possibility of using this biofunctionalized material for future biosensors.

1 Introduction

Porous silicon (PS) can be used as smart transducer material in sensing application particularly in the detection of vapors, liquids and biochemical molecules [1]. In fact, on exposure of chemical substances, several physical quantities such as refractive index, photoluminescence, and electrical conductivity change drastically [1, 2]. A key feature of a physical transducer, being sensitive to organic and biological molecules, either in vapor or liquid state is a large surface area of the order of 200–500 m^2 cm^{-3}, thus ensuring an effective interaction with several adsorbates [3]. Moreover, PS is available as a low cost material and is completely compatible with standard integrated circuit processes. Therefore, it could easily be employed in the so-called smart sensors [4]. Furthermore, PS technology has shown great capability in detecting biological molecules with high selectivity, using specific linker agent and probe molecules [5]. For the biomedical applications of PS, biomolecules have to be first immobilized on its surface through functional groups deposited on it. The common approach is to create a covalent bond between the PS surface and the biomolecules which specifically recognize the target analytes [5]. The reliability of a biosensor strongly depends on the functionalization process depending on its fastness, simplicity, homogeneity and its repeatability [6]. It is well known that after anodization, the fresh silicon surface is predominately hydride-terminated which is quite reactive and sensitive to oxidation [6]. Thus to increase the surface stability of PS, there is a need to functionalize the surface of PS by a suitable precursor.

In this work, nanostructured PS's surface was biofunctionalized by depositing on to its surface thin biocompatible films with a large density of amine groups, using 3-aminopropyltriethoxysilane (APTS) thermally. The choice of APTS as a functionalization material was based upon the fact that amine groups are present in proteins and their chemical interaction with other functional groups is well documented [2, 7]. The aim of the present study is to demonstrate the covalent bonding between organic molecules (immunoglobulin) and modified inorganic surface (nanostructure PS) which can be used for the detection of protein signals. The biofunctionalized surface of PS was characterized by different techniques like photoluminescence (PL), X-ray

S. Singh · S. N. Sharma (✉) · Govind · S. M. Shivaprasad · M. Lal
Electronic Materials Division, National Physical Laboratory, Dr. K·S. Krishnan Marg, New Delhi 110012, India
e-mail: shailesh@mail.nplindia.ernet.in

S. Singh · M. A. Khan
Faculty of Life Science, Aligarh Muslim University, Aligarh 202001, India

photoelectron spectroscopy (XPS) and Fourier transform Infrared (FTIR) spectroscopy respectively. The present work shows a potential approach to PS-based biosensors.

2 Experimental

Boron doped p type Si monocrystalline wafers of (100) orientation, 0.5 ± 0.5 Ω-cm resistivity and 400 ± 0.5 μm thickness were used for preparing PS. PS samples were formed by electrochemical etching using Si as the anode and Pt as the counter electrode in an acid-resistant Teflon container. A thin aluminum layer was evaporated on the back of the wafers and sintered to form an ohmic contact. The anodization was carried out at different current densities $I_d \sim 20$–70 mAcm^{-2} for 30 min, in a solution of H_2O: HF:IPA (1:1:2). After etching, the samples were rinsed with propanol and dried under a stream of dry high-purity nitrogen prior to use. In the present work, nano-structured PS surface was biofunctionalized by the deposition of APTS thermally at 100°C for about 4–5 h. The silane 3-APTS is one of the most common precursors which, by following the appropriate process, can leave amine groups (NH_2) available for reaction with either a cross-linking agent or directly with a molecule. The samples were thoroughly rinsed with propanol and dried under stream of pure nitrogen. The sample after APTS attachment was characterized by PL, FTIR and XPS. The functionalized PS were immersed into a solution of glutaraldehyde (2.5%) pH 7 which was used as a cross linker. The wafers were kept in the solution for 1 h at room temperature. It was important to rinse successively with DI water in order to remove all excess of glutaraldehyde. The antibody (Human IgG) (5 g/ml in acetic/acetate buffers, pH 5) was immobilized on treated PS surface. 0.1% bovine serum albumin (BSA) a blocking agent was incorporated also increase hydrophilicity. The substrates were cleaned with 0.05% Tween 20 in phosphate buffered saline (PBS) and put in contact with antigen (Goat anti Human IgG) for 1 h, then, rinsed with buffer (0.05% Tween 20 in PBS) solution for 30 min at room temperature [2] and finally rinsed with DI water.

The PL was measured using a home assembled system consisting of a two stage monochromator, a photomultiplier tube (PMT) with a lock-in amplifier for PL detection, and an Ar^+ ion laser operating at 488 nm and 5 mW (corresponding to 0.125 W cm^{-2}) power for excitation. FTIR spectra were recorded with a Perkin Elmer Model (Spectrum BX) spectrophotometer. XPS measurements were performed in an ultra-high vacuum chamber (PHI 1257) with a base pressure of $\sim 4 \times 10^{-10}$ torr. The XPS spectrometer is equipped with a high resolution hemispherical electron analyzer (279.4 mm diameter with 25 meV resolution) and a Mg (K_α) ($h\nu = 1253.6$ eV) X-ray excitation source.

3 Results and discussion

The porosity of PS films as estimated from gravimetric measurements [8] range from 68–95% corresponding to I_d varying from 20 to 70 mA cm^{-2}, respectively. Typical PL curves for PS films formed at different current densities I_d on unpolished substrates corresponding to electrolyte H_2O:HF:IPA (1:1:2) are shown in Fig. 1a. As evident from Fig. 1a, the absolute PL intensity is higher for PS formed at $I_d \sim 50$ mA cm^{-2} with $\lambda_{max} \sim 650$ nm (Fig. 1a, curve c). However, at further higher $I_d \sim 70$ mA cm^{-2}, the PL intensity decreases drastically (Fig. 1a, curve e). At this I_d, the films are powdery, non-adherent to the substrate and

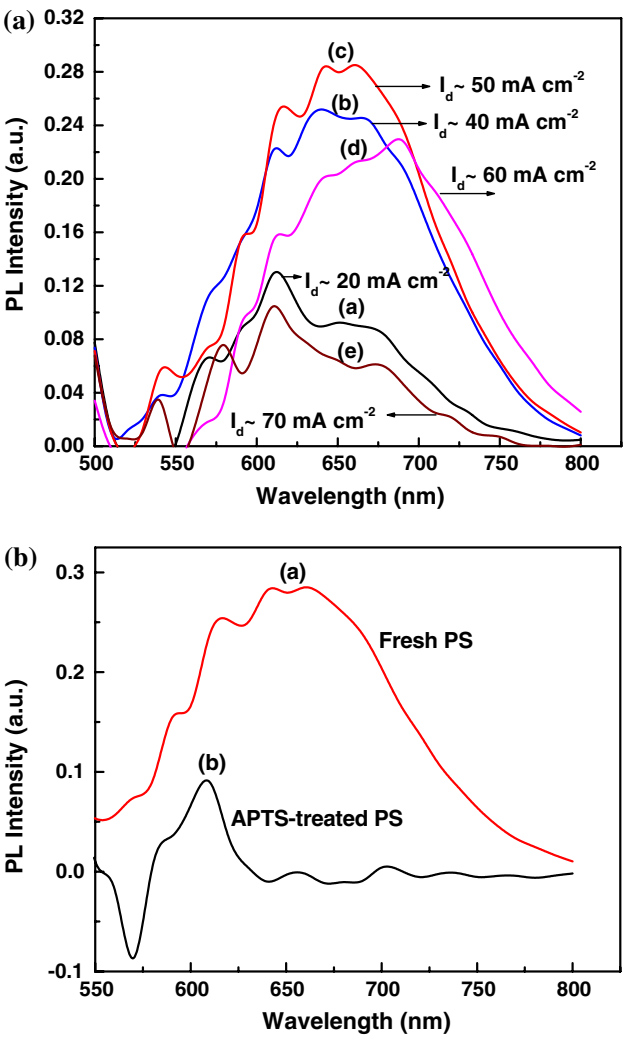

Fig. 1 (**a**) PL spectra of fresh PS prepared at different I_d (20–70 mA cm^{-2}), curves (a-e); (**b**) PL spectra of fresh PS (curve a) and APTS treated PS (curve b) prepared at $I_d \sim 50$ mA cm^{-2}

has a peeling-off tendency. At a lower $I_d \sim 20$ mA cm^{-2}, the PL intensity of PS film is low and PL intensity profile is quite similar to that obtained for $I_d \sim 70$ mA cm^{-2} ($\lambda_{max} \sim 612$ nm) (Fig. 1a, curves a & e). From Fig. 1a (curves a-d), with increase in current density from 20 to 60 mA cm^{-2}, the subsequent shift of the PL spectra from 612 to 690 nm (red-shift) with increment in PL intensity could be due to the effect of the oxide related species on the surface of PS as observed earlier [9]. This could be due to the breaking of Si–Si bonds with concomitant decrease in Si-skeleton size and formation of Si–O bonds [9]. The interface region being passivated by oxygen all the same, there was little drop in PL intensity with increase in I_d from 50 to 60 mA cm^{-2}. However, at further higher $I_d \sim 70$ mA cm^{-2}, due to excessive etching of the Si-skeleton, the PL intensity decreases significantly with concurrent PL blue-shift (Fig. 1a, curve e). Visual observation shows that the PS films at $I_d \sim 50$ mA cm^{-2}, appear more uniform and strong as compared to PS films formed at other I_d's. Thus, $I_d \sim 50$ mA cm^{-2}, is the optimized I_d where a higher PL intensity is obtained and silanization experiments (APTS treatment) and subsequent biomolecule (immunoglobulin) attachment is carried out.

Figure 1b shows PL spectra of fresh PS and APTS treated PS prepared at $I_d \sim 50$ mA cm^{-2} respectively. The APTS-treated PS film shows a PL quenching with considerable decrease in PL intensity. This irreversible quenching can be attributed to a chemical modification of the PS sample that generates non-radiative surface traps resulting in decrease in PL intensity upon APTS attachment [10]. It could also be due to energy or charge transfer from the PS to the APTS [11]. The fact that APTS is a charge acceptor provides an indication that the quenching of PL most probably occurs via a charge transfer mechanism. Presently, lifetime measurements of PS films in the presence of APTS films are carried out to ascertain the type of quenching mechanism.

Ideally the silanization process (APTS treatment) should occur without any oxidation of the PS surface. But experimentally, it has been observed that besides Si–H bonds, Si–Si bonds also break to some extent because of formation of SiO_2 during APTS decomposition and later deposition as also reported by others [12]. The concomitant shift of the PL peak position from 650 to 610 nm (blue-shift) upon APTS treatment for $I_d \sim 50$ mA cm^{-2} in Fig. 1b indicates breaking of Si–Si bonds and formation of Si–O bonds which causes reduction in Si-skeleton dimensions. It could also be due to the presence of the group (O–Si–CH_2–CH_2–CH_2–NH_2) which remains intact in most of the APTS molecules during the functionalization process [13].

Decay of PL intensity is a good indication of the stability of PS films particularly of surface bond configurations [14]. In Fig. 2a, decay of the PL intensity at the peak wavelength

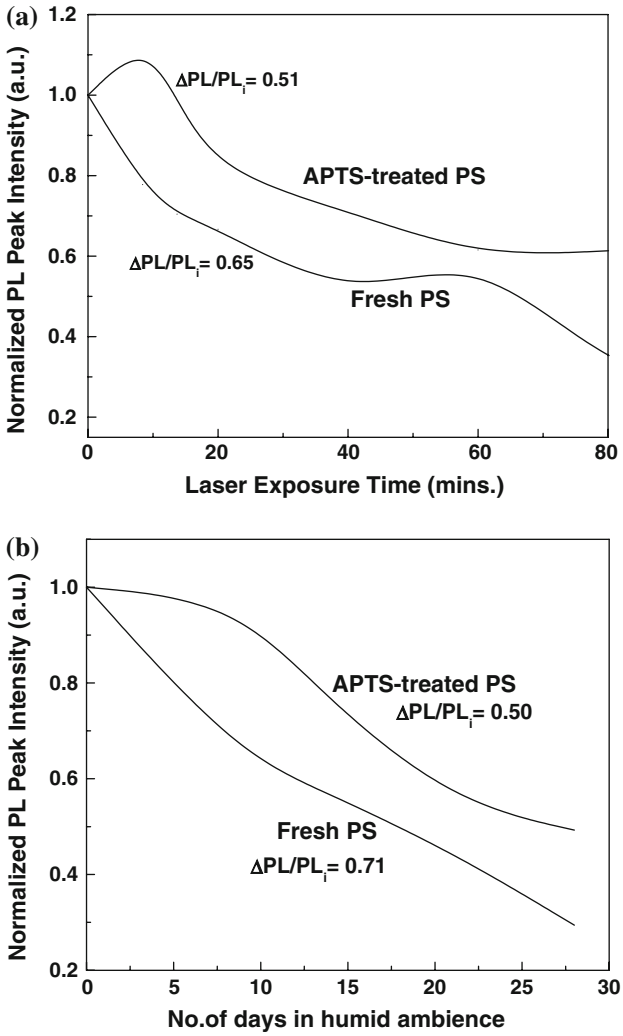

Fig. 2 PL decay of fresh PS and APTS-treated PS corresponding to $I_d \sim 50$ mA cm^{-2} under (**a**) normal-ambience; (**b**) humid-ambience

for PS films formed as such and APTS-treated PS at $I_d \sim 50$ mA cm^{-2}, are compared. The PL peak position was recorded for different times corresponding to a peak wavelength (λ_{max}). As shown in Fig. 2a, significant decay of the PL intensity is observed for fresh PS film as compared to the APTS treated one with rate of PL decay (ΔPL/PLi) being 0.65 and 0.51, respectively. In humid ambience, the rate of PL decay for fresh PS films is ∼0.71 while the rate of PL decay for APTS–treated PS is ∼0.50 (Fig. 2b).

From Fig. 2a and b, for APTS-treated PS film corresponding to $I_d \sim 50$ mA cm^{-2}, the initial increase in PL intensity during 10 min of laser or humid ambience exposure is either due to the adsorption of oxygen and/or water molecules, which reduces recombination from surface states, or a surface photo-oxidation, which can create an additional barrier for the carriers resulting in passivation of Si-dangling bonds [15]. Upon prolonged laser exposure, dangling bonds/defects are created due to the breaking of

Si–Si bonds and hence PL intensity decreases. Similar effect was also observed for fresh PS films after 50 min of laser or humid ambiance exposure (Fig. 2a and b). However, this effect is felt more for laser exposed PS samples as compared to the one subjected to humid ambiance due to the faster rate of oxidation associated with the former. To ensure the reproducibility of this PL decay, measurements were done repeatedly and for several hours and the PL decay trend was found to be the same. This is a direct evidence for the formation of stable surface and correlates with the superior mechanical stability of APTS-treated PS film as compared to fresh PS film prepared at $I_d \sim 50$ mA cm^{-2}.

Figure 3a shows the IR transmittance spectra of fresh PS and APTS-treated PS corresponding to $I_d \sim 50$ mA cm^{-2}. The fresh PS film exhibit Si–H related modes at $\sim$2105 cm^{-1} due to Si–H stretching mode, 900 cm^{-1} due to Si–H_2 scissors or Si–H_3 symmetric or anti-symmetric deformation, 795 and 640 cm^{-1} due to Si–H_2 and Si–H wagging, small peak at $\sim$2308 cm^{-1} could be related to O backbonded to Si in Si–H stretching mode, small peak at $\sim$2920 cm^{-1} could be due to C–H stretching modes [16, 17]. Here, incorporation of C could be due to a slight atmospheric contamination of freshly prepared PS. It is worthwhile to note that as prepared PS shows a weak signature of O atoms either bonded to Si at $\sim$1250 cm^{-1} or backbonded to SiH related modes at $\sim$2308 cm^{-1}. The presence of these FTIR peaks can be understood from the fact that at higher $I_d \sim 50$ mA cm^{-2}, the interface region is being passivated by oxygen and hence formation of Si–O related bonds which are in accordance with PL results as well. Upon treatment of PS film with APTS, the Si–H related modes at $\sim$640, 795, 900 and 2105 cm^{-1} as observed in fresh PS film completely vanishes (Fig. 3a). This observation implies a hydrosilylation reaction that consumes mainly Si–H bonds (preferentially SiH_2 and SiH_3) rather than cleaving Si–Si bonds alone as reported for the thermal reaction of alcohols [18] and Grignard [19] and alkyl lithium [20] reagents with PS. The FTIR of the APTS-treated PS film as shown in Fig. 3a shows presence of three new peaks viz. $\sim$2770 and 2983 cm^{-1} corresponding to vibrational bands of CH_2 [2, 21] and $\sim$1722 cm^{-1} corresponding to bending modes of NH_2 [2, 22] respectively. From Fig. 3a, it is evident that for APTS-treated PS, the absence of unreacted SiH bonds remaining on the surface after the thermal modification implies efficient coverage of amines (-NH_2) groups on PS surface. This result is in contrast with other reports where steric hindrance was observed upon introduction of the organic molecules thus resulting in insufficient coverage on the PS surface [23]. Moreover, upon APTS-treatment there was a slight increase of the Si–O related mode at $\sim$1216 cm^{-1} (Fig. 3a) indicating that the silanization does takes place

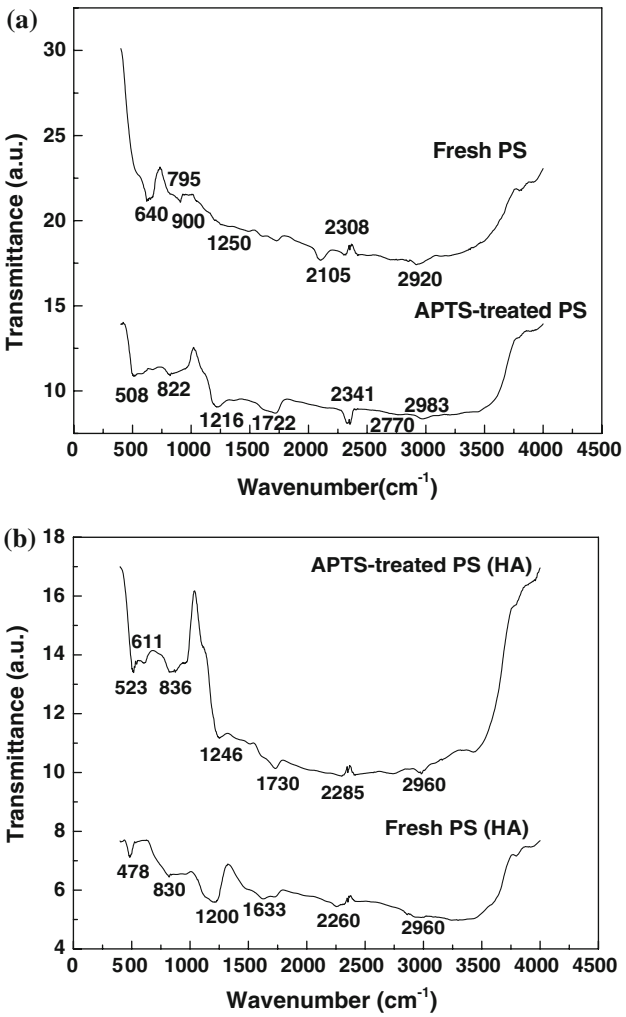

Fig. 3 FTIR transmittance spectra of fresh PS and APTS-treated PS corresponding to $I_d \sim 50$ mA cm^{-2} under (**a**) normal-ambience and (**b**) humid-ambience

but with slight oxidation of the PS surface presumably due to the formation of SiO_2-related species as reported by others as well [12].

Under humid ambience, the FTIR spectra of fresh PS film is appreciably affected with concomitant development of characteristic peaks of Si–O related modes with a doublet comprising of peak at $\sim$2260 cm^{-1} (O backbonded to Si in SiH stretching mode [16, 17], a distinct peak at $\sim$1200 cm^{-1} (Si–O-Si) stretching mode [16, 17] (Fig. 3b). The absence of Si–H related modes at $\sim$640 and $\sim$2100 cm^{-1} is also a testimonial to the formation of oxide species on the surface of fresh PS upon humid treatment. From Fig. 3a and b, the concurrent shift of Si–O related mode towards higher wave number from 1216 to 1246 cm^{-1} for APTS-treated PS films upon exposure to humid ambiance indicates marginal increment in the oxidation state of the SiO_x species [17] which is in agreement

with the above results. However, the APTS-treated PS films have high stability and its oxidation rate is relatively low as compared to fresh PS which again underlines the importance of chemical modification of the PS surface with APTS. Thus oxidation by means of humid conditions or laser exposure has no significant effect on the properties of APTS-treated PS films which shows the chemical stability and inertness of PS films upon APTS-treatment. These results are also supported by PL decay studies as well.

Figure 4a and b shows the full XPS survey spectra of fresh PS and APTS-treated PS films. The XPS spectra in Fig. 4a corresponding to fresh PS displays following peaks at 284.6, 531.7 and doublet at 99.0 and 102.9 eV corresponding to C (1 s), O (1 s) and Si (2p) [12, 23, 24], respectively. Upon APTS treatment, there is an increment in N(1 s) XPS signal at 401.3 eV [12] (Fig. 4b) as compared to the corresponding spectrum in Fig. 4a. This is due to incorporation of amines-NH_2 species on the surface of APTS-treated PS films. The XPS signals corresponding to C,O and Si can be seen at 284.6, 531.7 and 102.3 eV, respectively (Fig. 4b).

Figure 5a shows the Si (2p) core-level XPS spectra for fresh PS, APTS-treated PS and their corresponding spectra under humid ambience (HA). From Fig. 5a for fresh PS, the Si(2p) core level spectra shows the doublet at 99.0 and ~103 eV which indicates that Si exists in two different environments pure Si and oxidized Si [12, 25]. However, APTS-treated PS shows Si(2p) singlet peak at ~102.3 eV which indicates that for thermally treated PS sample for silanization, the entire PS surface is silanized with no evidence of any pure single crystal Si peak. This can be explained by the presence of SiO_2 or (O–Si–CH_2–CH_2–CH_2–NH_2) groups during thermal silanization experiment [13].

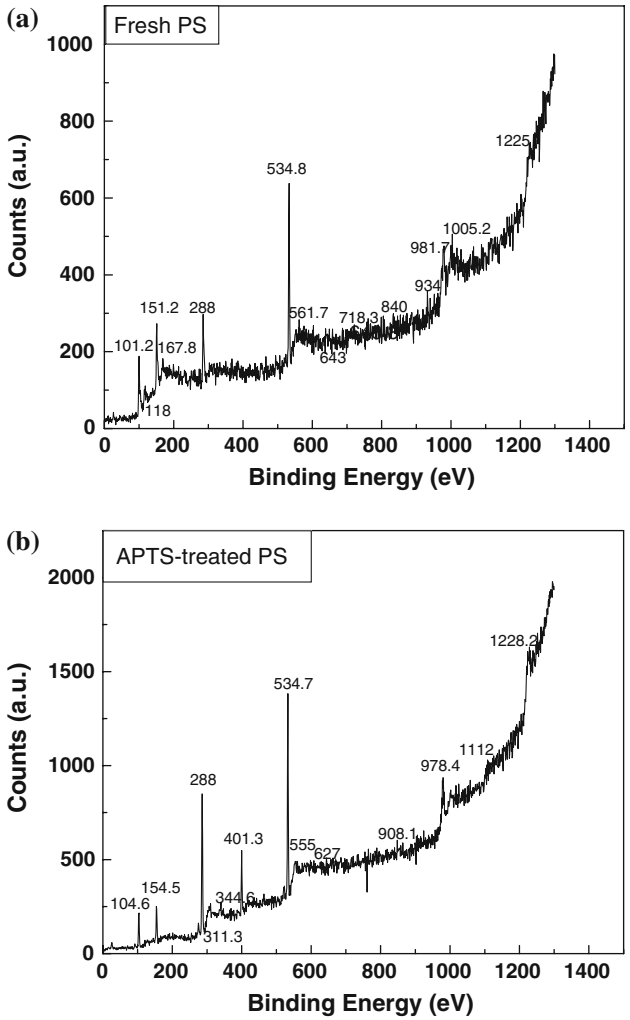

Fig. 4 XPS survey spectra corresponding to $I_d \sim 50$ mA cm^{-2} for (**a**) Fresh PS and (**b**) APTS-treated PS

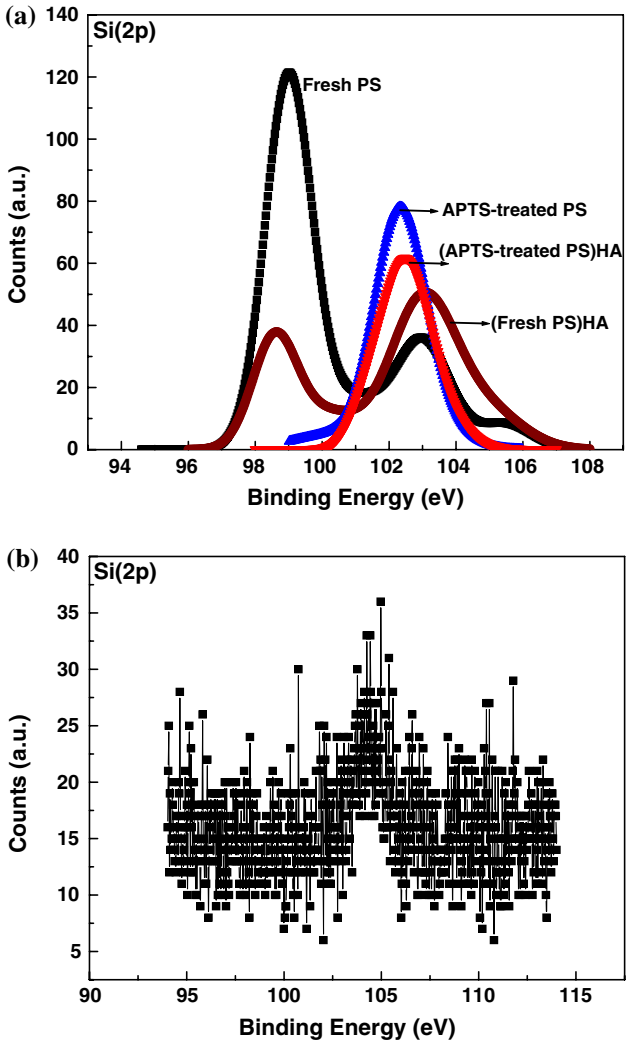

Fig. 5 XPS Si (2p) core-level spectra corresponding to $I_d \sim 50$ mA cm^{-2} for (**a**) fresh PS, APTS-treated PS and their corresponding spectra under humid ambience; and (**b**) upon immunoglobulin (Human IgG and Goat anti human IgG) attachment

Under humid ambience, the Si(2p) XPS peak intensity corresponding to pure Si(~99.0 eV) decreases drastically for fresh PS film as compared to APTS-treated PS film indicating higher degree of oxidation for fresh PS films as compared to APTS-treated PS film since SiO/Si (fresh PS) ≫>SiO/Si(APTS-treated PS) as evident from Fig. 5a. Upon oxidation, the rate of decrease of XPS signal for Si(2p) core level is significant for fresh PS as compared to APTS-treated PS which shows that APTS-treated PS films are relatively stable under oxidation conditions as also elucidated by PL decay and FTIR results respectively. The IgG molecules can be immobilized onto the surface of APTS-treated PS only than on fresh PS because of the presence of reactive NH_2 groups on treated sample as compared to the fresh one. When immunoglobulin ((Human IgG and Goat anti human IgG binding) are immobilized onto APTS-treated PS film, the Si (2p) peak almost disappeared and showed a weak signal (Fig. 5b). The disappearance of the Si(2p) peak suggests that the thickness of the antibody layer and the APTS layer must have exceeded the escape depth of Si(2p) electron and is a proof of protein adsorption.

From O(1 s) core level spectra (Fig. 6a), both fresh PS and APTS-treated PS films in normal ambience exhibit similar oxidation features (similar XPS peak intensity at ~531.7 eV) but under humid ambience, O(1 s) peak corresponding to fresh PS shifts to higher binding energy (~532.2 eV) while O(1 s) core-level intensity and peak position remains the same for APTS-treated PS film indicating higher level of oxidation for the former than for the latter. Figure 6b shows the corresponding C(1 s) core-level XPS spectra, where the fresh PS films exhibits lower C content as compared to APTS-treated PS film which can be attributed to an increase in C- and N-like species upon silanization for APTS-treated film. However, under humid ambience, C(1 s) core-level intensity decreases marginally for APTS-treated PS film whereas the fresh PS film shows a considerable increment in C(1 s) XPS intensity possibly resulting from the atmospheric carbon contamination. From Fig. 6c corresponding to N (1 s) core level XPS spectra, the increment in N-signal with similar peak position indicates increment in NH_2 species on the surface of PS which renders it quite stable and resistant to oxidation. This is not so in the case of untreated i.e., fresh PS film. When immunoglobulin ((Human IgG and Goat anti human IgG binding) are immobilized onto APTS-treated PS film, the N(1 s) and C(1 s) peak intensity increases (Fig. 6b and c). The enhancement of the nitrogen and carbon content was due to the immobilization of the protein. In the case of N(1 s) core level XPS spectra (Fig. 6c), the peak position at ~399.0 eV for APTS-treated PS, corresponding sample under humid condition and upon immunoglobulin attachment clearly shows the presence of $–NH_2$ species [26, 27].

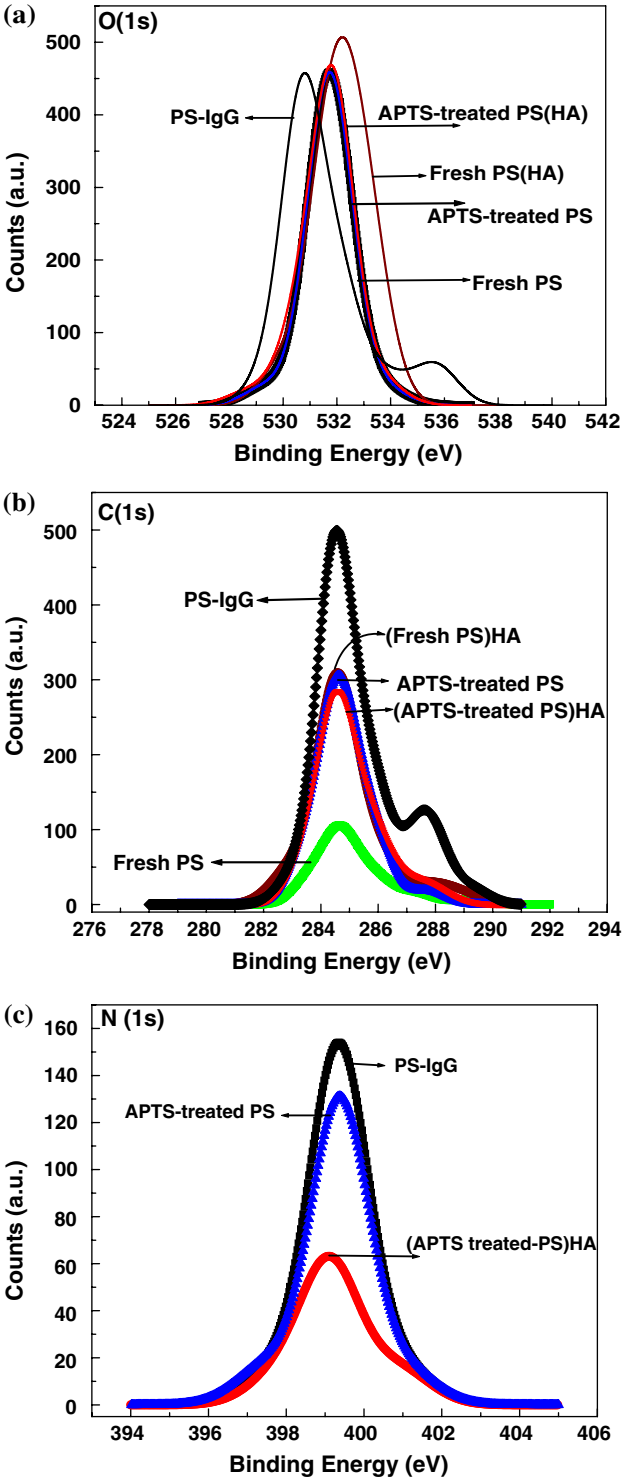

Fig. 6 XPS core-level spectra corresponding to I_d ~ 50 mA cm^{-2} for fresh PS, APTS-treated PS and their corresponding spectra under humid ambience and upon immunoglobulin (Human IgG and Goat anti human IgG) attachment; (**a**) O(1s); (**b**) C(1s) and (**c**) N(1s)

The absence of higher binding energy component here implies absence of any decomposition product of the APTS precursor. The increase in the width of the C(1 s) XPS

core-level spectrum with subsequent development of extra peak at 287.6 eV (C–N species) (Fig. 6b) and disappearance of Si(2p) XPS signal (Fig. 5b) upon IgG attachment is a proof of protein adsorption [26, 27]. Thus the results of XPS proved conclusively that the antibodies were site directly immobilized onto the APTS-treated PS surface.

4 Conclusions

A simple silanization with a three-step reaction has been developed to link biomolecules to PS surfaces. PS films prepared at an optimized $I_d \sim 50$ mA cm^{-2}, having high PL intensity, stable surface bond configurations, mechanically strong structure and hydrogen-passivated surfaces essentially conforms its viability for the effective biofunctionalization using APTS as precursor which ensures covalent linking between the surface and biomolecules. The PL, FTIR and XPS characterization demonstrated the presence of amine groups for APTS-treated PS films. Finally, it has been shown that antibodies can be immobilized on biofunctionalized PS maintaining their native character. The ease of this method of biofunctionalization and low cost technique opens the possibility of using biofunctionalized PS in biosensing devices.

Acknowledgements We thank Director NPL for the encouragement to perform this work. Shalini Singh gratefully acknowledges CSIR (New Delhi) for SRF fellowship.

References

1. L. De Stefano, L. Moretti, I. Rendina, A.M. Rossi, S. Tundo, Appl. Opt. **43**, 167 (2004)
2. O. Meskini, A. Abdelghani, A. Tlili, R. Mgaieth, N. Jaffrezic-Renault, C. Martelet, Talanta **71**, 1430 (2007)
3. L. De Stefano, L. Moretti, A.M. Rossi, M. Rocchia, A. Lamberti, O. Longo, P. Arcari, I. Rendina, IEEE Trans. Nanotech. **3**, 49 (2004)
4. H. Ouyang, C.C. Striemer, P.M. Fauchet, Appl. Phys. Lett. **88**, 163108 (2006)
5. L. Mongo, G. Vasapollo, M.R. Guascito, C. Malitesta, Anal. Bioanal. Chem. **385**, 146 (2006)
6. L. De Stefano, L. Rotiroti, I. Rea, L. Moretti, G.D.I. Francia, E. Massera, A. Lamberti, P. Arcari, C. Sanges, I. Rendina, J. Opt. A: Pure Appl. Opt. **8**, S 540 (2006)
7. D.C. Tessier, S. Boughaba, M. Arbour, P. Roos, G. Pan, Sensor. Actuat. B. **120**, 220 (2006)
8. O. Bisi, S. Ossicini, L. Pavesi, Surf. Sci. Rep. **38**, 1 (2000)
9. S.N. Sharma, G. Bhagavannarayana, Umesh Kumar, R. Debnath, S. Chandramohan, Physica E: Low-dimensional Syst Nanostruct **36**(1), 65 (2007)
10. S.E. Letant, B.R. Hart, S.T.A.C.I.R. Kane, M.Z. Hadi, S.J. Shields, J.G. Reynolds, Adv. Mater. **16**, 689 (2004)
11. M.P. Stewart, J.M. Buriak, Adv. Mater. **12**, 859 (2000)
12. M.A. Hernandez, R.J.M. Palma, J.P. Rigueiro, J.P. Garcia-Ruiz, J.L. Garcia-Fierro, J.M.M. Duart, Mat. Sci. Eng. C **23**, 697 (2003)
13. P.X. Zhu, Y. Masuda, K. Koumoto, J. Colloid Interface Sci. **243**, 31 (2001)
14. S.N. Sharma, G. Bhagavannarayana, R.K. Sharma, S.T. Lakshmikumar, Mat. Sci. Eng. B **127**, 255 (2006)
15. A.A. Bol, A. Meijerink, J. Phys. Chem. B **105**, 10203 (2001)
16. S.N. Sharma, R.K. Sharma, S.T. Lakshmikumar, Physica E **28**, 264 (2005)
17. S.N. Sharma, R. Banerjee, D. Das, S. Chattopadhyay, A.K. Barua, Appl. Surf. Sci. **182**, 333 (2001)
18. N.Y. Kim, P.E. Laibinis, J. Am. Chem. Soc. **119**, 2297 (1997)
19. N.Y. Kim, P.E. Laibinis, J. Am. Chem. Soc. **120**, 4516 (1998)
20. J.H. Song, M.J. Sailor, J. Am. Chem. Soc. **120**, 2376 (1998)
21. B. Xia, S.J. Xiao, D.J. Guo, J. Wang, J. Chao, H.B. Liu, J. Pei, Y.Q. Chen, Y.C. Tang, J.N. Liu, J. Mater. Chem. **16**, 570 (2006)
22. H.L. Li, A.P. Fu, D.S. Xu, G.L. Guo, L.L. Gui, Y.Q. Tang, Langmuir **18**, 3198 (2002)
23. R. Boukherroub, S. Morin, D.D.M. Wayner, D.J. Lockwood, Solid State Commun. **118**, 319 (2001)
24. Q. Weiping, X. Bin, Y. Danfeng, L. Yihua, W. Lei, W. Chunxiao, Y. Fang, L. Zhuhong, W. Yu, Mat. Sci. Eng. C **8–9**, 475 (1999)
25. T.V. Torchinskaya, N.E. Korsunskaya, L.Y.U. Khomenkova, B.R. Dhumaev, S.M. Prokes, Thin Solid Films **381**, 88 (2001)
26. Y. Wang, S. Han, A.L. Briseno, R.J.G. Sanedrin, F. Zhou, J. Mater. Chem. **14**, 3488 (2004)
27. S. Sharma, R.W. Johnson, T.A. Desai, Biosens. Bioelectron. **20**, 227 (2004)